processes

Article

Research on Response Characteristics and Control Strategy of the Supercritical Carbon Dioxide Power Cycle

Chunhui Dai [1,2], Ping Song [1,2,*], Can Ma [1,2], Kelong Zhang [1,2], Wei Zheng [1,2], Lie Chen [1,2], Xiaojie Guo [1,2], Yuansheng Lin [1,2] and Zhiqiang Qiu [1,2]

1 Key Laboratory of Thermal Power Technology, Wuhan 430064, China; ch.dai@163.com (C.D.); macan1234@sina.com (C.M.); sworkcsic@163.com (K.Z.); zhengwei@mail.ustc.edu.cn (W.Z.); helloworldum@163.com (L.C.); lucky_gxj_0372@163.com (X.G.); keylab_rndl@163.com (Y.L.); jchdlzhjs@126.com (Z.Q.)

2 Wuhan Second Ship Design and Research Institute, Wuhan 430064, China

* Correspondence: pingsong@stu.xjtu.edu.cn

Abstract: With the development of GEN-IV nuclear reactor technology, the supercritical carbon dioxide (SCO_2) Brayton cycle has attracted wide attention for its simple structure and high efficiency. Correspondingly, a series of research has been carried out to study the characteristics of the cycle. The control flexibility of the power generation system has rarely been studied. This paper carried out a dynamic performance of the 20 MW-SCO_2 recompression cycle based on the Simulink software. In the simulation, the response characteristics of the system main parameters under the disturbances of cooling water temperature, split ratio, main compressor inlet temperature and pressure were analyzed. The results show that the turbine inlet temperature is most affected by the disturbances, with a re-stabilization time of 2500–3000 s. According to the response characteristics of the system after being disturbed, this study proposed a stable operation control scheme. The scheme is coordinated with the main compressor inlet temperature and pressure control, recompressor outlet pressure control, turbine inlet temperature control and turbine load control. Finally, the control strategy is verified with the disturbance of reduced split ratio, and the results show that the control effect is good.

Keywords: supercritical carbon dioxide Brayton cycle; Simulink; disturbance; control strategy

check for updates

Citation: Dai, C.; Song, P.; Ma, C.; Zhang, K.; Zheng, W.; Chen, L.; Guo, X.; Lin, Y.; Qiu, Z. Research on Response Characteristics and Control Strategy of the Supercritical Carbon Dioxide Power Cycle. *Processes* **2021**, *9*, 1943. https://doi.org/10.3390/pr9111943

Academic Editor: Pei Liu

Received: 2 September 2021
Accepted: 27 October 2021
Published: 29 October 2021

1. Introduction

The supercritical carbon dioxide (SCO_2) Brayton cycle has been widely used in a variety of power generation scenarios, including nuclear energy [1], solar energy [2], and thermal power [3]. The concept of SCO_2 Brayton cycle can be traced back to the 1960s [4]. With the development of the GEN-IV nuclear reactor, the SCO_2 Brayton cycle attracted attention from all over the world for its simple structure and high efficiency. Scholars also proposed the latest advancement of Allam cycle power generation technologies, making the CO_2 available at pipeline specification [5,6] and the corresponding dynamic simulation and control strategies were also studied [7,8], which directly promoted the sequestration and utilization of SCO_2.

Correspondingly, a series of research has been carried out to study the characteristics of the cycle [9–12]. However, most of the existing SCO_2 cycle studies are limited to basic thermodynamics research, parameter optimizations, and system design in different application fields. Considering that the SCO_2 cycle is widely used in the power generation system, attention needs to be paid to the performance of variable load and flexibility. Thus, the research on its dynamic model and control strategy is also essential, but this part of the work is still in infancy.

Hu et al. [13] carried out dynamic modeling on the recuperator of a 2 MW-SCO_2 power generation system, and mainly studied the fluid parameter change law in the recuperator during cold start and variable load. Ma et al. [14] developed the dynamic model of the recuperators for the 1000 MW-SCO_2 coal-fired power unit and analyzed the parameter dynamic response trend with the inlet temperature and mass flow rate change. Then, the neural network was trained to predict the performance of the Printed Circuit Heat Exchanger (PCHE). Due to the difficulty in manufacturing SCO_2 compressors and turbines, especially for high-load power generation systems, some scholars fitted empirical formulas and expanded the scale based on the performance curves of the existing SCO_2 turbomachines, aiming to increase the performance prediction accuracy of CO_2 rotating machinery under non-design conditions, such as Cho et al. [15] and Lee et al. [16].

As for the overall system, Dyreby [17] provided a detailed SCO_2 system modular modeling method and principles under non-design conditions, including the modeling methods of key components and the solution process of the overall system, but there was little analysis on the system dynamic performance. Zhu [18] developed a 350 kW SC recompression closed-loop dynamic model with Panysimu software and analyzed the main parameter response characteristics under the disturbance of the heat source duty, regulating valve opening and cooling water flow, but the research on the control strategy was not conducted.

Luu et al. [19] proposed a combined start-up control scheme of the simple recuperation cycle and recompression cycle with the background of solar energy applications. The simple recuperation cycle was applied to meet the design point at the initial start-up period, and then the system was merged into the recompression branch after the stable operation for 1 h. The total start-up time is about 4 h. As opposed to Luu's combined branch startup program, Liese et al. [20] adopted an inventory control scheme to directly adjust the system flow through the storage tank and realize the startup, shutdown and load tracking condition switch of the recompression system, which can shorten the startup and shutdown time. At the same time, the study pointed out that the model of the cooler should be at least one-dimensional.

In addition to the start-stop control scheme, the control strategy for the stable operation of the system has also been preliminary studied. Olumayegun et al. [21] studied the operation control strategy of the waste heat recovery system. The simulation results pointed out that the turbine inlet temperature should change with the change of waste heat, but the model was developed as an open loop. Sun [22] developed a closed-loop dynamic model of the system against the background coal-fired power generation and compared the effects of the constant flow control strategy and the constant turbine inlet temperature control strategy. The results pointed out that the former had stable control effects, while the latter had a higher cycle efficiency, especially under low-load operating conditions. The study by Du et al. [23] also reached the same conclusion.

Overall, part of the existing research mainly focused on the component level and some studies provided general modeling methods and dynamic responses to parameter disturbances. Moreover, the existing control strategy research mainly pays attention to the system start-stop plan. Thus, there is a lack of research on the dynamic characteristics of SCO_2 cycle and the control strategy for stable operation. As a supplement to the previous research, this paper studies the dynamic performance of the SCO_2 recompression cycle based on a 20 MW sodium-cooled reactor with Simulink software. This study mainly analyzes the dynamic response characteristics of the recompression cycle with the disturbances of cooling water temperature, split ratio, main compressor inlet temperature and pressure, which have been rarely studied previously. According to the response characteristics, a control strategy for the stable operation of the system is proposed and the split ratio disturbance is verified.

2. Simple Description of System

2.1. Comparison of Typical SCO_2 Cycles

Numerous layouts of the SCO_2 Brayton cycle have been researched. Typically, simple cycle, simple recuperated cycle and recompression cycle are included in the general SCO_2

Brayton cycle. Figures 1–3 shows the three-type cycle diagram and T-s curve respectively, where T means temperature and s means entropy. What's more in the T-s curves, the Brayton cycle thermodynamic process are presented and the numbers mean the sequence of the process.

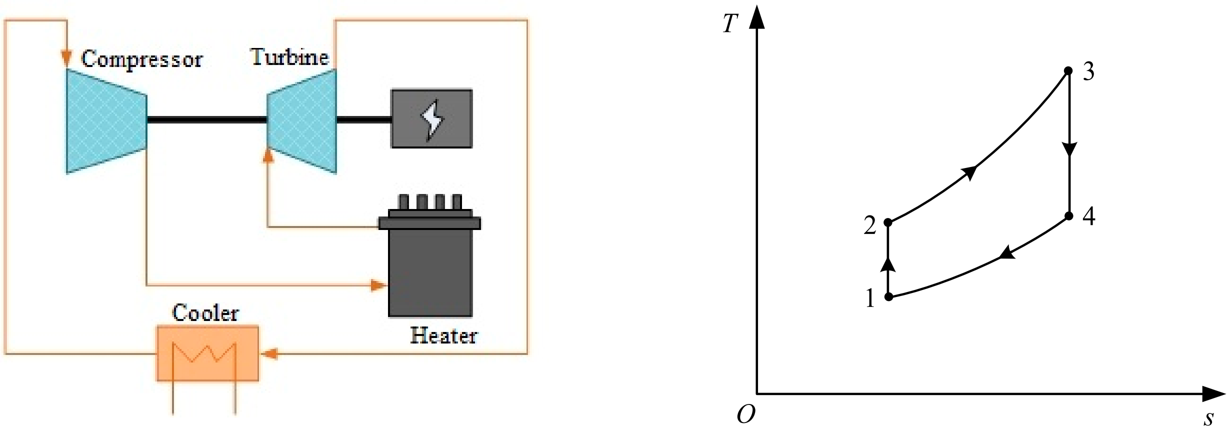

(**a**) cycle diagram (**b**) T-s curve

Figure 1. SCO_2 simple cycle.

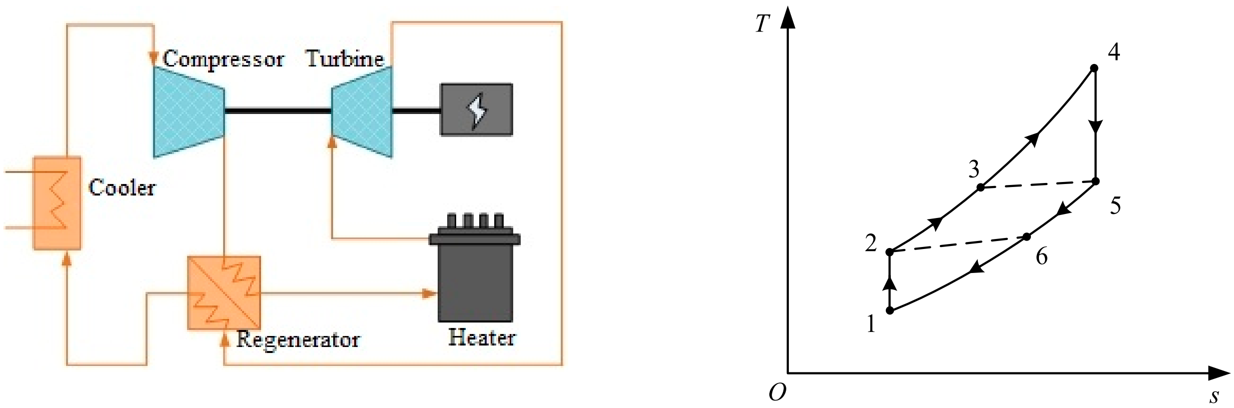

(**a**) cycle diagram (**b**) T-s curve

Figure 2. SCO_2 simple recuperated cycle.

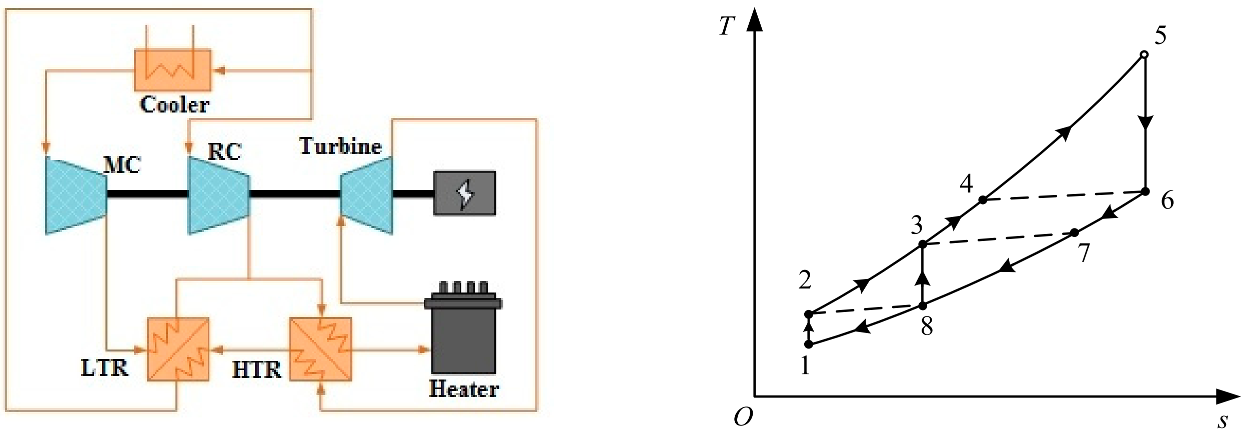

(**a**) cycle diagram (**b**) T-s curve

Figure 3. SCO_2 recompression cycle.

The SCO_2 simple cycle is based on the typical Brayton cycle principle. The included compressor, heater, turbine and cooler correspond to the Brayton cycle thermodynamic process of isentropic compression (point1 to point 2 in Figure 1b), constant pressure heat absorption (point 2 to point 3 in Figure 1b), adiabatic expansion (point 3 to point 4 in Figure 1b) and constant pressure release (point 3 to point 4 in Figure 1b), as shown in Figure 1. In the simple SCO_2 cycle system, the low-temperature and low-pressure SCO_2 enters the heater to absorb heat after being boosted by the compressor, and then the high-temperature and high-pressure SCO_2 enters the turbine to perform work. Finally, the exhausted SCO_2 flows into the compressor through the cooler. Thus, a closed cycle is completed. Part of the turbine output power is used to drive the compressor to pressurize the SCO_2, and the rest drives the generator to generate electricity. Given that the physical properties of SCO_2 change drastically near the critical point, the density is relatively large, and the compression coefficient is relatively small, the compressor consumes less power. Moreover, the back pressure of turbine and the exhausted SCO_2 temperature are relatively high, and the direct heat release in the cooler causes a large amount of heat loss, so the efficiency of the SCO_2 simple cycle is extremely low.

The simple recuperated cycle arranges a regenerator based on the simple cycle, as shown in Figure 2. The high-temperature exhausted SCO_2 from the turbine is used to preheat the low-temperature SCO_2 from the compressor outlet. Thus, part of the exhausted heat is recovered and the energy loss of the cooler is reduced. At the same time, the heat absorption temperature of SCO_2 at the inlet of the heater is increased, and the heat absorption of the cycle is reduced, so the cycle efficiency is improved.

Due to the large difference in temperature and pressure of SCO_2 on both sides of the regenerator, the difference in the specific heat capacity is obvious. Meanwhile, the flow rate of the fluid on both sides is equal and the heat capacity is quite different. The above factors result in the pinch point of the regenerator, which will have a great impact on the cycle efficiency.

The SCO_2 recompression cycle solves the pinch point problem of the simple recuperated cycle by adding the thermal process of split flow and recompression, as shown in Figure 3. With the design of split flow, the regenerator is divided into two stages. On the one hand, the temperature change on both sides of the high-temperature regenerator is small. On the other hand, the flow rate of the low-temperature fluid in the low temperature regenerator becomes less after the split, and the heat capacity is reduced. Thus, the high and low temperature regenerators are not prone to the problem of pinch points. Meanwhile, the split circulation sacrifices part of the work to compress the fluid, so that the fluid temperature is increased after being reheated. The heat absorption at the heater is reduced under the same conditions, and the heat loss of the pre-cooling is reduced, which improves the cycle efficiency.

2.2. Description of Recompression System

Considering the problem of the pinch point in the simple recuperated cycle, the power generation system described in this paper adopts the SCO_2 recompression cycle, and the configuration is shown in Figure 4. A small part of the supercritical carbon dioxide is separated and compressed in the RC, and the other is still compressed in the MC. The regenerator is divided into two stages. This can effectively avoid the pinch point of the regenerator. The overall system includes turbine (T), main compressor (MC), recompressor (RC), high-temperature and low-temperature recuperators (HTR and LTR), intermediate heat exchanger (IHE), pre-cooler (PC), surge tank (ST) and heater.

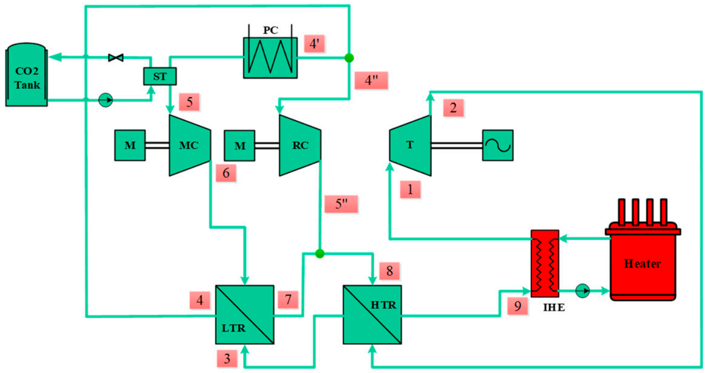

Figure 4. Supercritical carbon dioxide recompression cycle power generation system.

The closed-loop system model was debugged and the initial operating parameters were calculated. The Simulink configuration diagram is shown in Figure 5. The heat duty is inputted to the system to simulate the heater at a value of 64.3 MW. The SCO_2 in the IHE absorbs the heat and flows into the turbine to do work. After the heat release in the HTR and LTR, with a given split ratio (*SR*) at 0.3852, about 38.52% of the SCO_2 flows into the RC to be compressed directly. The rest is cooled in the PC and compressed in the MC. Then, the two streams converge at the outlet of the high-pressure side of LTR and continually flow into the HTR and IHE. Thus, an integral process is completed. The input parameters of the design condition are shown in Table 1.

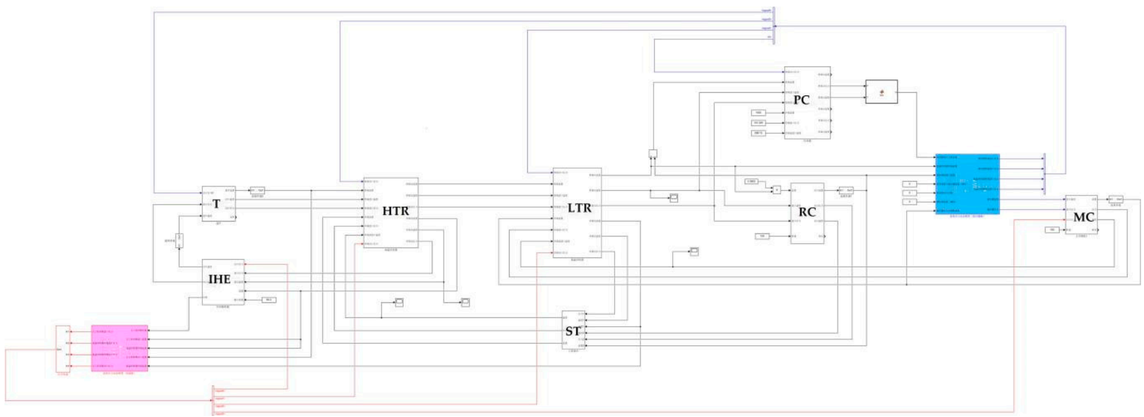

Figure 5. Simulink dynamic model diagram of SCO_2 recompression cycle.

Table 1. Input parameters under design condition of recompression cycle model.

Input Parameters	**Values**
Rotating speed of MC\% Design rotating speed	100
Rotating speed of RC\% Design rotating speed	100
Spilit ratio	0.3853
Cooling water temperature\K	304.4
Cooling water mass flow rate\kg/s	1400
Cooling water pressure\MPa	0.101
Heater duty\MW	64.3

Based on the developed dynamic model of the 20 MW-SCO_2 recompression cycle with Simulink software, this paper studied the response characteristics and control strategy of the SCO_2 recompression cycle.

3. Disturbance Analysis

In this paper, the response characteristics of the SCO_2 recompression system with the disturbances of cooling water temperature, split ratio (*SR*), MC inlet pressure and temperature were first analyzed.

3.1. Cooling Water Temperature

The cooling water is obtained from outside in the actual operation. On the one hand, if the water temperature is too high, the CO_2 cannot be cooled to the design temperature, which will reduce the cycle efficiency; on the other hand, the water temperature being too low may cause the CO_2 to exit the supercritical state, resulting in the system failing to operate normally. Therefore, the cooling water temperature disturbance is simulated and analyzed in this section. In the simulation, the compressor and turbine run at a constant rotating speed, the cooling water flow rate and the heater duty remain unchanged, while the cooling water temperature steps up by 2 K. The simulation results are shown in Figure 6.

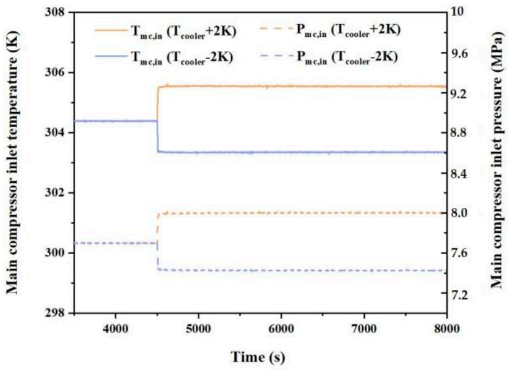

(**a**) MC inlet parameters

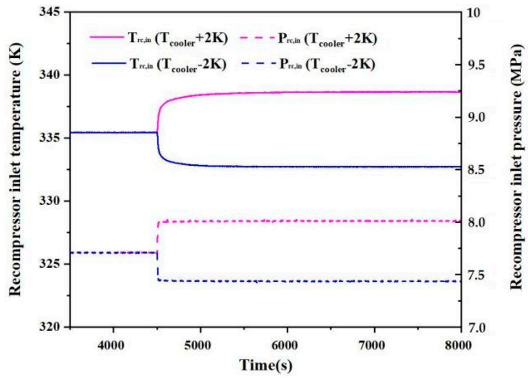

(**b**) RC inlet parameters

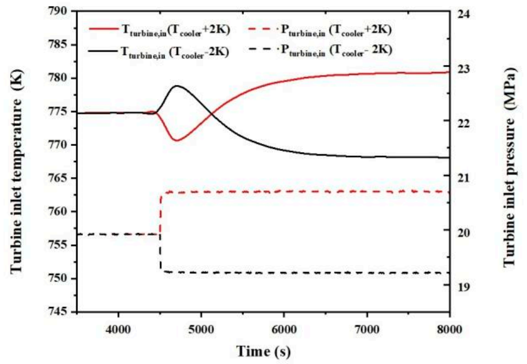

(**c**) Turbine inlet parameters

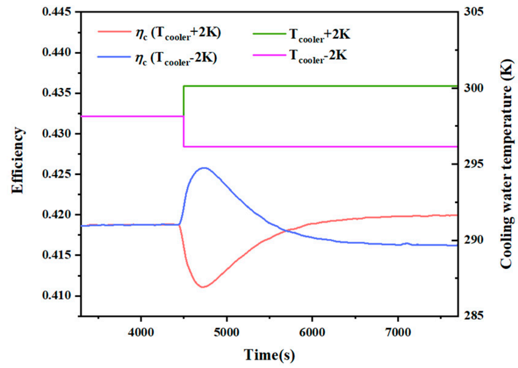

(**d**) Efficiency

Figure 6. Response curves of main parameters with cooling water temperature disturbance.

As can be seen from Figure 6, the MC inlet temperature is the first to be affected, rising by about 1.1 K and showing an approximate step change with the cooling water temperature stepping up by 2 K. Figure 6b shows that the RC inlet temperature increases by about 3.1 K, and the time for re-stabilization is about 1500 s. In Figure 6c, the inlet temperature of turbine decreases first and then increases, and the variation range is about 6 K. Due to the strong coupling of the closed-loop system and the thermal inertia of the HTR and LTR, the re-stabilization time of the turbine inlet temperature is as long as 3000 s. The volume of each component is lumped in the ST and IHE for the integral calculation of the density and enthalpy, and the physical property software is applied to calculate the pressure change of the working fluid. Pressure responds very quickly to the system disturbance, and the pressure at the key points of the system shows an approximate step change. Compared with the design conditions, the MC inlet pressure increased by about 0.3 MPa and the turbine inlet pressure increased by about 0.77 MPa. Under the disturbance of the cooling water temperature, the cycle efficiency change and the turbine inlet temperature change show the same trend as shown in Figure 6d. When the cooling water temperature steps down by 2 K, the parameters change laws are opposite to the above.

3.2. Split Ratio (SR)

The split ratio was used to express the share of flow entering the RC. The low-pressure side outlet fluid of the LTR is divided into two streams: one stream is cooled in the PC and then compressed in the MC, while the other stream is directly compressed in the RC. Under the premise of the design condition, assuming that the split ratio (*SR*) steps up by 0.01 (from 0.3853 to 0.3953) at 4500 s, other input parameters of the system remain unchanged. The system is simulated and the results are shown in Figure 7.

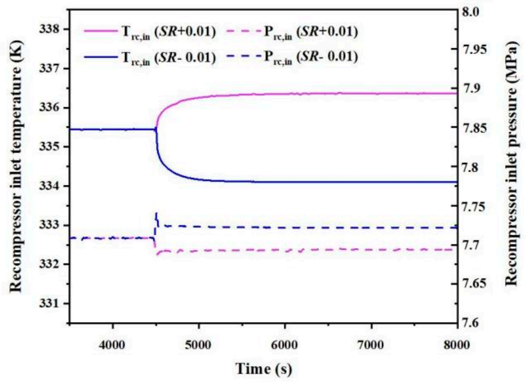

(**a**) RC inlet parameters

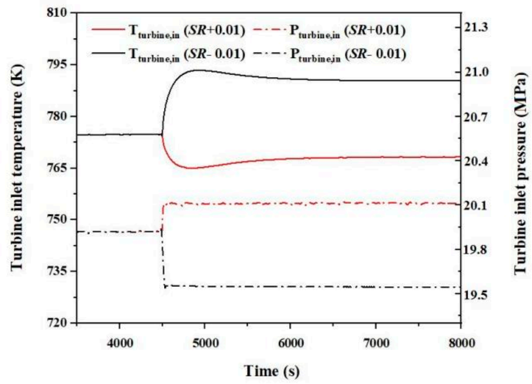

(**b**) Turbine inlet parameters

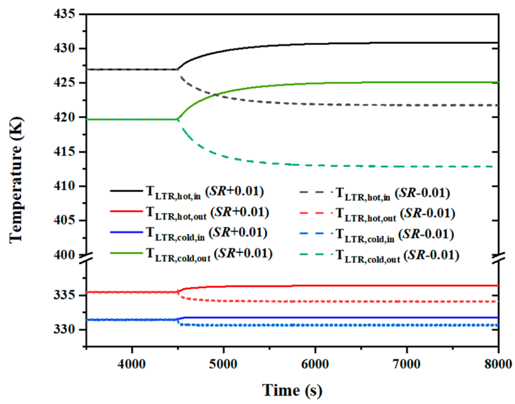

(**c**) LTR inlet and out temperatures

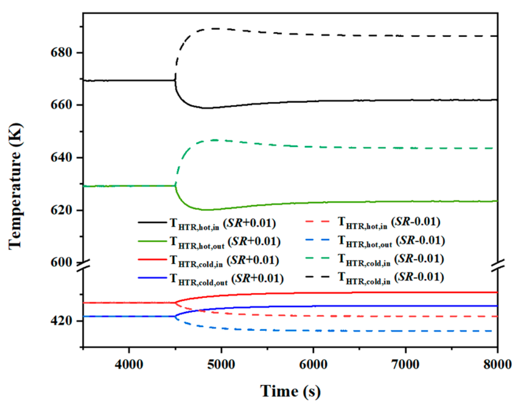

(**d**) HTR inlet and out temperatures

Figure 7. Response curves of main parameters with *SR* disturbance.

When the split ratio steps up by 0.01, the temperature and pressure at the inlet of MC change slightly. The RC inlet temperature increases by about 1.0 K, and the time for re-stabilization is about 1500 s (Figure 7a). On the contrary, the inlet temperature of the turbine decreases by about 6.4 K, while the re-stabilization time after disturbance is as long as about 2500 s (Figure 7b). These changes are triggered by the change of the mass flow rate in each branch. The mass flow rate of the working fluid at the MC and the cold end of LTR decreases as the split ratio increases, so the temperature of the working fluid at the hot end outlet of the LTR and the inlet of RC increases. At this time, both the inlet and outlet temperatures of the LTR increase (Figure 7c). However, the disturbance of *SR* increases the CO_2 flow rate in the main circuit. When the heater duty is constant, the turbine inlet temperature decreases. Correspondingly, the temperatures at the hot end inlet and cold end outlet of the HTR decrease (Figure 7d). Under the disturbance of the split ratio, the pressures of the system change rapidly, and behave similarly to the step responses. Specifically, the RC inlet pressure decreases and the turbine inlet pressure increases.

When the split ratio steps down by 0.01, the parameter variation trends are opposite to the above and the parameter change ranges are large.

3.3. MC Inlet Pressure

In this simulation, the MC inlet pressure steps up by 0.2 MPa (from 7.7 to 7.9 MPa) at 4500 s with the premise of the design condition, and the other input parameters of the system remain unchanged. The system simulation was carried out and the results are shown in Figure 8.

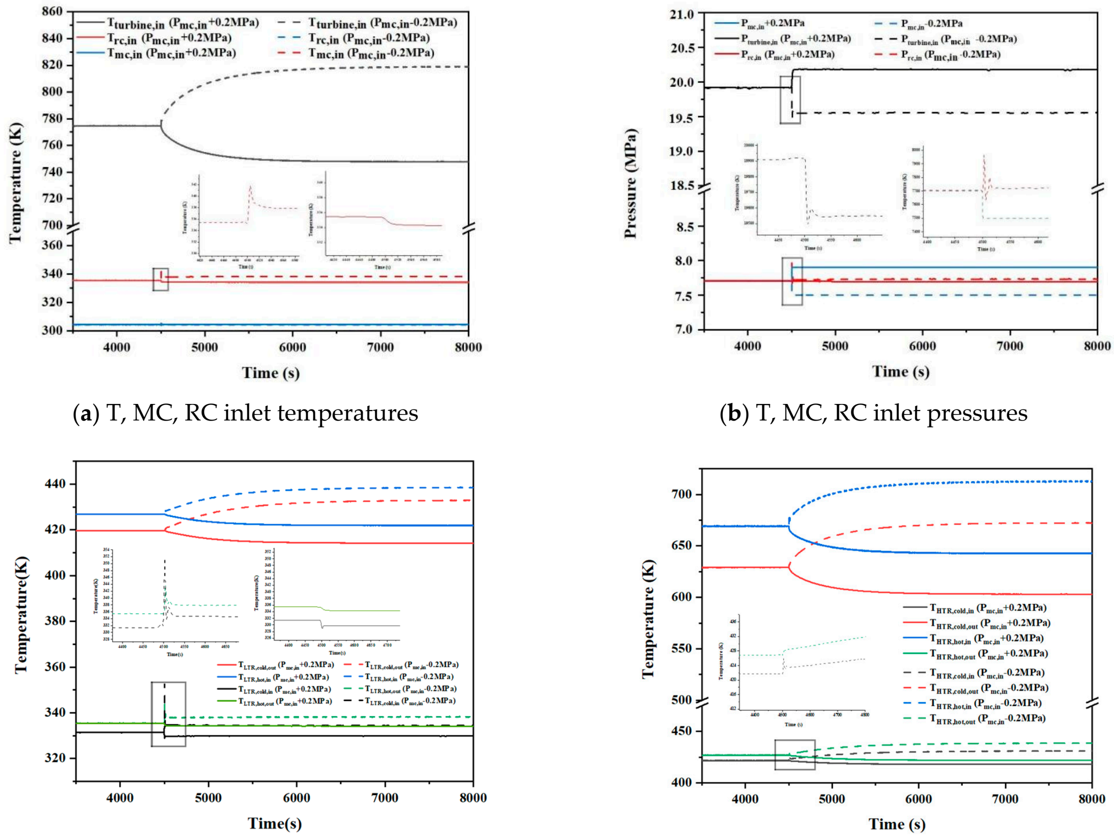

(**a**) T, MC, RC inlet temperatures (**b**) T, MC, RC inlet pressures

(**c**) LTR inlet and out temperatures (**d**) HTR inlet and out temperatures

Figure 8. Response curves of main parameters with MC inlet pressure disturbance.

When the MC inlet pressure steps up by 0.2 MPa, the MC inlet temperature changes slightly, the RC inlet temperature decreases by about 1.3 K, and the re-stabilization time is about 80 s. The inlet temperature of the turbine is greatly affected by the disturbance of the MC inlet pressure, which is reduced by about 26.2 K, and the re-stabilization time is as long as 2500 s (Figure 8a). Because of the rapid response of pressure, the turbine inlet pressure increases by 0.25 MPa, which shows an approximate step change. Instead, the RC inlet pressure is almost constant (Figure 8b). As the MC inlet pressure increases, the MC outlet temperature decreases, and thus the inlet and outlet temperatures of LTR and HTR decrease. The temperature re-stabilization time of each point on the recuperator cold side increases with the flow direction of low-temperature CO_2, while the temperature re-stabilization time of each point on the hot side of the recuperators decreases with the flow direction of high-temperature CO_2 (Figure 8c,d).

When the MC inlet pressure steps down by 0.2 MPa, the parameters change trend are opposite to the above and the parameters change ranges are larger. It is worth noting that when the MC inlet pressure is reduced from 7.7 to 7.5 MPa, the pressure at this point is closer to the critical pressure. The pressures and temperatures of some key points of the system will fluctuate for a short time, such as the RC inlet temperature and pressure responses. In addition, the LTR cold end inlet temperature and hot end outlet temperature response may even cause the deterioration of LTR heat transfer, as shown in Figure 8c.

3.4. MC Inlet Temperature

In the SCO_2 recompression system, the MC inlet temperature and pressure need to stay above the critical point. However, when the system is disturbed by the split ratio, cooling water temperature and mass flow rate, the MC inlet temperature may drop below the critical point. Therefore, this section will discuss the dynamic characteristics of the system main parameters when the MC inlet temperature drops below the critical point.

Assuming that the MC inlet temperature is stepped down by 1.0 K (from 304.4 to 303.4 K) at 4500 s with the premise of the design condition, and other input parameters of the system remain unchanged. The system was simulated and the results are shown in Figure 9. When the MC inlet temperature steps down by 1.0 K, the RC inlet temperature decreases by about 2.7 K and the time for re-stabilization is about 500 s. As shown in Figure 9a, the inlet temperature of the turbine is greatly affected by the disturbance of the MC inlet temperature, which is reduced by about 15 K, and the re-stabilization time is as long as 3000 s. The temperature of each point of the recuperators decreases accordingly as the disturbance occurs. The temperature re-stabilization time of each point on the recuperator cold side increases with the flow direction of low-temperature CO_2; the temperature re-stabilization time of each point on the hot side of the recuperators decreases with the flow direction of high-temperature CO_2, as shown in Figure 9b,c.

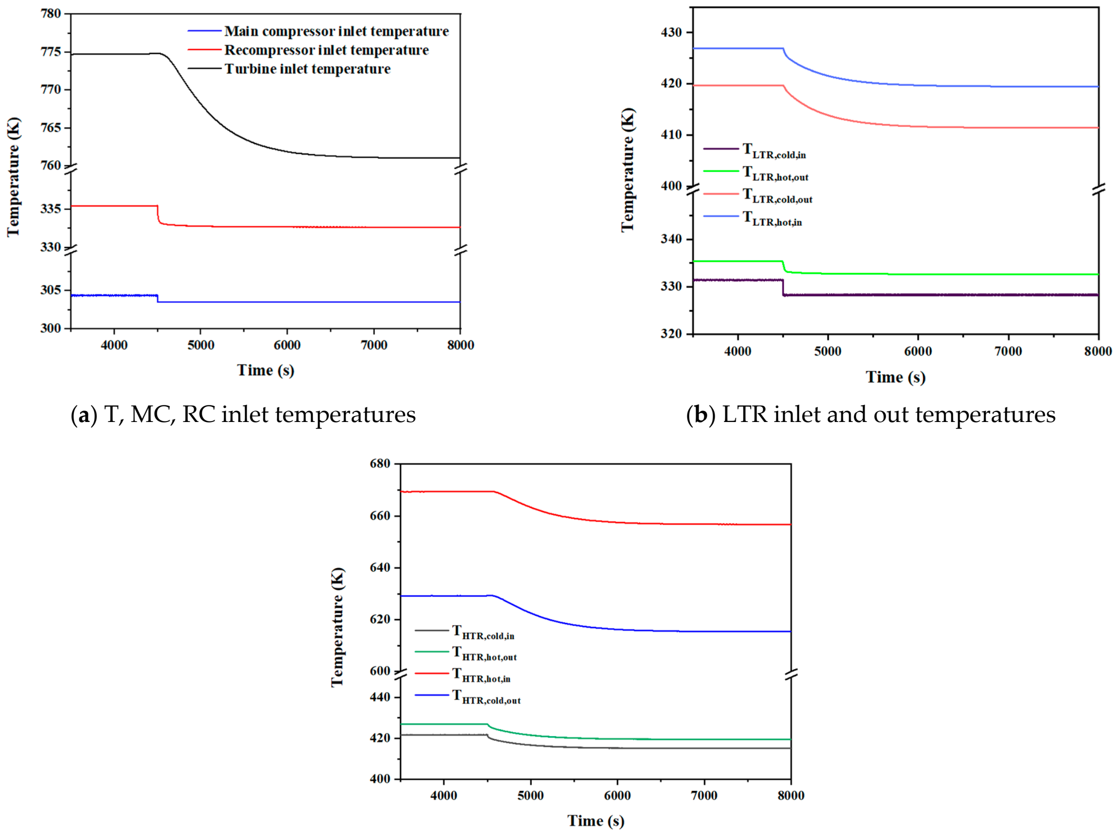

(**a**) T, MC, RC inlet temperatures (**b**) LTR inlet and out temperatures

(**c**) HTR inlet and out temperatures

Figure 9. Response curves of main parameters with MC inlet temperature disturbance.

4. Control Strategy of Stable Operation

The control strategy for the stable operation was proposed based on the response characteristics. Finally, the system control effects with the disturbance of the split ratio were verified.

4.1. Control Strategy

From the above disturbances simulation results, it can be seen that the turbine inlet temperature is the most sensitive parameter to all disturbances, with large fluctuation range and long re-stabilization time. Therefore, this study adopts the stable operation control strategy and maintains the turbine inlet temperature constant. The overall control system is divided into the following five parts, as shown in Figure 10:

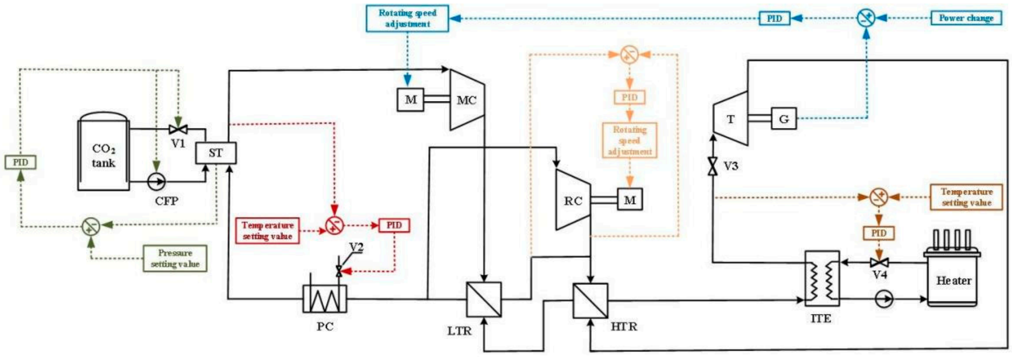

Figure 10. The operation control strategy of the SCO_2 recompression system.

The operation control strategy also consists of five parts: MC inlet pressure control module, MC inlet temperature control module, turbine inlet temperature control module, turbine output power control module and RC outlet pressure control module.

1. MC inlet pressure control module

The ST is connected to the front pipeline of the MC and the CO_2 storage tank, and its function is to maintain the MC inlet pressure at the set value, so the ST pressure is used as the controlled parameter. When the ST pressure is higher than the set value, the PRV (V1) is opened to draw a part of the working fluid from the ST, thereby reducing the pressure in the surge tank. When the ST pressure is lower than the set value, the CFP is ran to fill the CO_2 with specific parameters into the ST, thereby increasing the pressure in the ST.

2. MC inlet temperature control module

The MC inlet temperature was controlled to the set value by changing the cooling water flow rate. When the MC inlet temperature is higher than the set value, the difference signal between the MC inlet temperature and the set value is converted into a signal of the opening of the cooling water valve (V2) by the PID controller. The cooling water mass flow rate is increased by increasing the valve opening, thereby reducing the MC inlet temperature to achieve control effect. When the MC inlet temperature is lower than the set value, the control command is opposite.

3. Turbine inlet temperature control module

In order to reduce the influence of disturbance on the system, it is necessary to control the turbine inlet temperature. The turbine inlet temperature is controlled to the set value by changing the hot fluid mass flow rate of the ITE. When the turbine inlet temperature is lower than the set value, the difference signal between the turbine inlet temperature and the set value is converted into a signal of opening the valve (V4) by the PID controller. The hot fluid mass flow rate of ITE increases with the increase of the valve opening, and thus the turbine inlet temperature will decrease. When the turbine inlet temperature is higher than the set value, the control command is opposite.

4. Turbine output power control module

The system flow is changed by adjusting the rotating speed of the MC to realize the turbine load tracking in this study. When the turbine load demand changes, the difference signal between the demand value and the current turbine load is transmitted to the PID controller, and then converted into a variable frequency signal of the MC rotating speed by the PID controller. The MC speed increases as the turbine load demand increases, and vice versa. The system flow rate changes with the MC rotating speed, and finally the turbine load is adjusted to meet the demand.

5. RC outlet pressure control module

In order to ensure that the pressure of the RC outlet working fluid is consistent with the LTR cold end outlet working fluid when they merge, the RC outlet pressure is taken as the controlled parameter. The RC flow rate is determined by the main circuit flow rate and the split ratio, so the outlet pressure can be adjusted by the rotating speed. The difference signal between the LTR cold end outlet pressure and the RC outlet pressure is transmitted to the PID controller and then converted into a frequency conversion signal of the RC rotating speed, which can realize the control function.

4.2. Control Effect Analysis

This section discusses the control effect with the disturbance of the split ratio. The split ratio is stepped down by 0.01 (decreased from 0.3853 to 0.3753) at 4500 s when operating under design condition. The PID parameter tuner of Simulink is used to tune the controller parameters.

In the SCO_2 system, considering that the MC inlet parameters must be kept above the critical point, the MC inlet temperature control has the highest priority in the coordinated control of the overall system. Because the turbine inlet temperature has a greater influence on the turbine power, the control command for the turbine inlet temperature is also faster than the mass flow rate control command using the power difference as a signal. The above is achieved by tuning the PID controller parameters.

The main control parameters and the response of the controlled quantity are shown in Figure 11. When the split ratio is stepped down, the recompressor flow rate decreases accordingly. The MC mass flow rate is controlled by the rotating speed and exhibits hysteresis, so the working fluid of the main circuit is reduced, and the output power of the turbine is also decreased. In the control system, the turbine output power demand remains unchanged, while the actual output is reduced. Thus, the signal of the difference is transmitted to the MC through the PID controller, and the mass flow rate control system starts to work then. The MC flow rate is increased with the increase of the MC rotating speed. The flow rate of the main circuit returns to the initial state in about 130 s, and the flow rate of each branch reaches the distribution balance under the new split ratio. During this period, the heater load and the cooling water mass flow rate are adjusted to maintain the turbine inlet temperature and MC inlet temperature at the set value. The MC inlet temperature is the first to return to the set value, and the fluctuating range of the turbine inlet temperature is ± 5 K, as shown in Figure 11c,d. With the cooperation of all control modules, the turbine power is almost restored to the demand value synchronously with the flow rate of the main circuit, and the control effects are good.

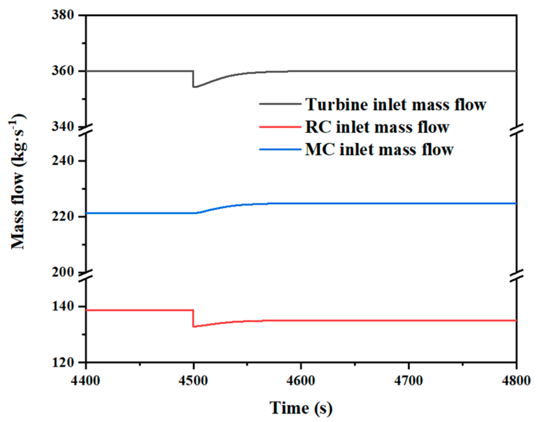

(**a**) System mass flow

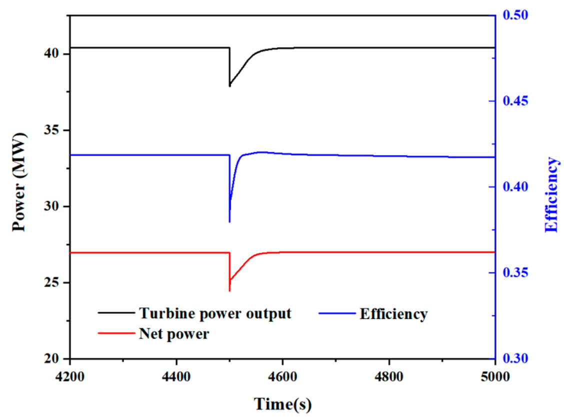

(**b**) Power and efficiency

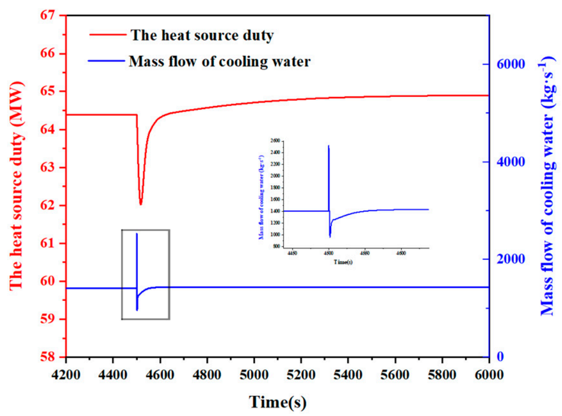

(**c**) The heater duty and flow of cooling water

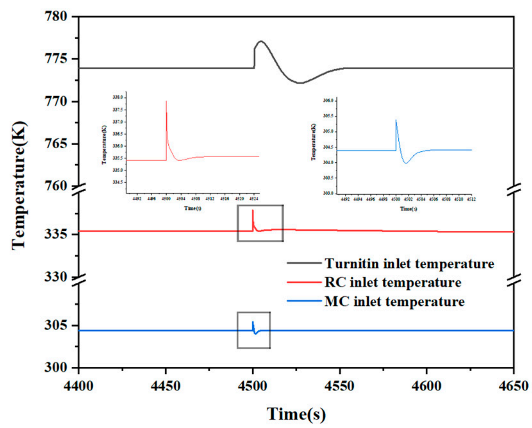

(**d**) T, MC, RC inlet temperatures

Figure 11. Response curves of controlled parameter with *SR* disturbance.

5. Conclusions

In this study, the response characteristics of the SCO_2 recompression cycle system were analyzed on the disturbances of cooling water temperature, split ratio, main compressor inlet temperature and pressure. Subsequently, according to the response characteristics of the system, a control strategy of stable operation was proposed. The verification effect of the split ratio disturbance was carried out to provide a reference for future SCO_2 dynamic research. The main conclusions of the study are as follows:

- When the system is subjected to a step disturbance, the pressure shows a similar step response rapidly, while the temperature change is relatively slow, especially for the turbine inlet temperature. Due to the closed-loop system features and the recuperator thermal inertia, the turbine inlet temperature fluctuates in a wide range and the re-stabilization time is the longest, about 2500–3000 s. The inlet temperature of the MC is easily reduced to below the critical point in the cooling water parameters disturbance, but adjusting the cooling water flow is an effective way to control the MC inlet temperature to be constant.
- For the split ratio disturbance and the MC inlet pressure disturbance, the reduction of the value has a greater impact on the system parameters than the increase of the value. When the MC inlet pressure is reduced from 7.7 to 7.5 MPa, the pressure at this point is closer to the critical pressure. The pressures and temperatures of the system key points will fluctuate for a short time, especially the LTR cold end inlet temperature and hot end outlet temperature responses, which may even cause the deterioration of LTR heat transfer.

- According to the response characteristics of the system after being disturbed, this study proposed a stable operation control scheme to coordinate the MC inlet temperature and pressure control, PC outlet pressure control, turbine inlet temperature control and turbine load control. When the split ratio decreases by 0.01, the parameters deviate from the set values and the turbine output power decreases. After the control system acts on for about 130 s, the flow rate of each branch reaches the distribution balance under the new split ratio, and meanwhile the turbine load returns to the set demand. The MC inlet temperature is the first to return to the set value, and the fluctuating range of the turbine inlet temperature is ±5 K. In general, the overall control effect is good.

Author Contributions: Conceptualization, K.Z.; Formal analysis, L.C.; Investigation, P.S.; Methodology, C.M.; Project administration, Y.L. and Z.Q.; Software, W.Z. and X.G.; Writing—original draft, P.S.; Writing—review and editing, C.D. All authors have read and agreed to the published version of the manuscript.

Funding: This research was funded by National Key R&D Program of China, grant number 2019YFB1901201.

Conflicts of Interest: The authors declare no conflict of interest.

References

1. Li, H.; Fan, G.; Cao, L.; Yang, Y.; Yan, X.; Dai, Y.; Zhang, G.; Wang, J. A comprehensive investigation on the design and off-design performance of supercritical carbon dioxide power system based on the small-scale lead-cooled fast reactor. *J. Clean. Prod.* **2020**, *256*, 120720. [CrossRef]
2. Qiao, Z.; Cao, Y.; Li, P.; Wang, X.; Romero, C.E.; Pan, L. Thermoeconomic analysis of a CO_2 plume geothermal and supercritical CO_2 Brayton combined cycle using solar energy as auxiliary heat source. *J. Clean. Prod.* **2020**, *256*, 120374.
3. Guo, J.; Li, M.; Xu, J.; Yan, J.; Ma, T. Energy, exergy and economic (3E) evaluation and conceptual design of the 1000 MW coal-fired power plants integrated with S-CO_2 Brayton cycles. *Energy Convers. Manag.* **2020**, *211*, 112713. [CrossRef]
4. Liu, M.; Yang, K.; Zhang, X.; Yan, J. Design and optimization of waste heat recovery system for supercritical carbon dioxide coal-fired power plant to enhance the dust collection efficiency. *J. Clean. Prod.* **2020**, *275*, 122523. [CrossRef]
5. Allamab, R.; Martin, S.; Forrest, B.; Fetvedt, J.; Lu, X.; Freed, D.; Brown, G.W., Jr.; Sasaki, T.; Itoh, M.; Manning, J. Demonstration of the Allam cycle: An update on the development status of a high efficiency supercritical carbon dioxide power process employing full carbon capture. *Energy Procedia* **2017**, *114*, 5948–5966. [CrossRef]
6. Fernandes, S.; Wang, Q.; Xu, B.R.; Chen, D. Process and carbon footprint analyses of the Allam cycle power plant integrated with an air separation unit. *Clean Technol.* **2019**, *1*, 325–340. [CrossRef]
7. Fernandes, D.; Wang, S.; Xu, Q.; Chen, D. Dynamic Simulations of the Allam Cycle Power Plant Integrated with an Air Separation Unit. *Int. J. Chem. Eng.* **2019**, *10*, 6035856 . [CrossRef]
8. Xiong, J.; Zhao, H.; Chen, H.; Zheng, C. Dynamic simulation of a conceptual 600 MWe oxy-fuel combustion power plant. In Proceedings of the 3rd Oxyfuel Combustion Conference, IEAGHG, Wuhan, China, 9–13 September 2013.
9. Sarkar, J. Second law analysis of supercritical CO_2 recompression Brayton cycle. *Energy* **2009**, *34*, 1172–1178. [CrossRef]
10. Ahn, Y.; Bae, S.J.; Kim, M.; Cho, S.K.; Baik, S.; Lee, J.I.; Cha, J.E. Review of supercritical CO_2 power cycle technology and current status of research and development. *Nucl. Eng. Technol.* **2015**, *47*, 647–661. [CrossRef]
11. Persichilli, M.; Kacludis, A.; Zdankiewicz, E.; Held, T. Supercritical CO_2 Power Cycle Developments and Commercialization: Why sCO_2 can Displace Steam Ste. *Power-Gen India Cent. Asia* **2012**, *2012*, 19–21.
12. Ma, Y.; Liu, M.; Yan, J.; Liu, J. Thermodynamic study of main compression intercooling effects on supercritical CO_2 recompression Brayton cycle. *Energy* **2017**, *140*, 746–756. [CrossRef]
13. Hu, H.; Guo, C.; Cai, H.; Jiang, Y.; Liang, S.; Guo, Y. Dynamic characteristics of the recuperator thermal performance in a S–CO_2 Brayton cycle. *Energy* **2021**, *214*, 119017. [CrossRef]
14. Ma, T.; Li, M.; Xu, J.; Cao, F. Thermodynamic analysis and performance prediction on dynamic response characteristic of PCHE in 1000 MW S-CO_2 coal fired power plant. *Energy* **2019**, *175*, 123–138. [CrossRef]
15. Cho, S.K.; Lee, J.; Lee, J.I. Off design performance map similarity study of radial type turbomachinery in supercritical co brayton cycle. In Proceedings of the Asme-jsme-ksme Joint Fluids Engineering Conference, Seoul, Korea, 26–31 July 2015.
16. Lee, J.; Ahn, Y.; Jung, H.Y. Off design performance of compressors of 150MWe S-CO_2 Cycle for Sodium Cooled Fast Reactor. In Proceedings of the Transactions of the Korean Nuclear Society Spring Meeting, Jeju, Korea, 29–30 May 2014.
17. Dyreby, J.J. *Modeling the Supercritical Carbon Dioxide Brayton Cycle with Recompression*; ProQuest Dissertations Publishing: Morrisville, NC, USA, 2014.
18. Zhu, Y. Research on Dynamic Characteristics of Supercritical Carbon Dioxide Brayton Cycle System. Master's Thesis, North China Electric Power University, Beijing, China, 2018.

19. Luu, M.T.; Milani, D.; McNaughton, R.; Abbas, A. Dynamic modelling and start-up operation of a solar-assisted recompression supercritical CO_2 Brayton power cycle. *Appl. Energy* **2017**, *199*, 247–263. [CrossRef]
20. Liese, E.; Albright, J.; Zitney, S.A. Startup, shutdown, and load-following simulations of a 10 MWe supercritical CO_2 recompression closed Brayton cycle. *Appl. Energy* **2020**, *277*, 115628. [CrossRef]
21. Olumayegun, O.; Wang, M. Dynamic modelling and control of supercritical CO_2 power cycle using waste heat from industrial processes. *Fuel* **2019**, *249*, 89–102. [CrossRef]
22. Jia, S. Characteristic Simulation and Control of Supercritical Carbon Dioxide Cycle Power Generation System. Master's Thesis, Harbin Institute of Technology, Harbin, China, 2018.
23. Du, X.; Hu, J.; Xia, G. Operation characteristic of supercritical carbon dioxide-cooled reactor system under coordination control scheme. *Int. J. Adv. Robot. Syst.* **2020**, *17*, 172988142093383. [CrossRef]